



ELSEVIER

Available online at www.sciencedirect.com

ScienceDirect

Proceedings of the Combustion Institute 000 (2022) 1–9

Proceedings
of the
Combustion
Institutewww.elsevier.com/locate/proci

A reactive molecular dynamics study of NO removal by nitrogen-containing species in coal pyrolysis gas

Zhongze Bai^a, Xi Zhuo Jiang^{b,*}, Kai H. Luo^{a,*}^a Department of Mechanical Engineering, University College London, Torrington Place, London WC1E 7JE, UK^b School of Mechanical Engineering and Automation, Northeastern University, Shenyang, Liaoning 110819, China

Received 29 December 2021; accepted 15 July 2022

Available online xxx

Abstract

Coal splitting and staging is a promising technology to reduce nitrogen oxides (NO_x) emissions from coal combustion through transforming nitrogenous pollutants into environmentally friendly gasses such as nitrogen (N₂). During this process, the nitrogenous species in pyrolysis gas play a dominant role in NO_x reduction. In this research, a series of reactive force field (ReaxFF) molecular dynamics (MD) simulations are conducted to investigate the fundamental reaction mechanisms of NO removal by nitrogen-containing species (HCN and NH₃) in coal pyrolysis gas under various temperatures. The effects of temperature on the process and mechanisms of NO consumption and N₂ formation are illustrated during NO reduction with HCN and NH₃, respectively. Additionally, we compare the performance of NO reduction by HCN and NH₃ and propose control strategies for the pyrolysis and reburn processes. The study provides new insights into the mechanisms of the NO reduction with nitrogen-containing species in coal pyrolysis gas, which may help optimize the operating parameters of the splitting and staging processes to decrease NO_x emissions during coal combustion.

© 2022 The Author(s). Published by Elsevier Inc. on behalf of The Combustion Institute.

This is an open access article under the CC BY license (<http://creativecommons.org/licenses/by/4.0/>)**Keywords:** NO reduction; Coal pyrolysis gas; Molecular dynamics; Reactive force field

1. Introduction

Nitrogen oxides (NO_x) from coal combustion cause serious environmental problems such as photochemical smog and acid rain [1]. To protect the environment from pollution, a variety of technolo-

gies for reducing NO_x emissions from coal combustion have been developed. Fuel staging or reburning is a well-know technology for NO_x reduction, where the NO_x emissions are reduced to N₂ by the injection of reburn fuels into the flue gas downstream of the combustion zone [2].

Many fuels have been investigated as reburn fuels during coal combustion such as natural gas [3], oil [4], coal [5] and coal pyrolysis gas [6,7]. Among them, coal pyrolysis gas, also called fuel splitting and staging, has better performance in NO_x reduction than other fuels [6,7]. In this process, coal is separated into char and pyrolysis gas through

* Corresponding author at: University College London, Department of Mechanical Engineering, Torrington Place, London WC1E 7JE, UK.

E-mail addresses: jiangxz@mail.neu.edu.cn (X.Z. Jiang), k.luo@ucl.ac.uk (K.H. Luo).

<https://doi.org/10.1016/j.proci.2022.07.154>

1540-7489 © 2022 The Author(s). Published by Elsevier Inc. on behalf of The Combustion Institute. This is an open access article under the CC BY license (<http://creativecommons.org/licenses/by/4.0/>)

Please cite this article as: Z. Bai, X.Z. Jiang and K.H. Luo, A reactive molecular dynamics study of NO removal by nitrogen-containing species in coal pyrolysis gas, Proceedings of the Combustion Institute, <https://doi.org/10.1016/j.proci.2022.07.154>

pyrolysis process first. The char burns in the main zone to release heat and generate NO_x. Pyrolysis gas is injected downstream of the main zone to create a fuel rich reburning zone, where NO_x is transformed into N₂. After the reburning zone, additional air is provided to ensure complete combustion of remaining fuel fragments. Previous studies [3–5] have identified that the nitrogenous species in pyrolysis gas are important for NO_x reduction performance in the coal splitting and staging process. Therefore, it is of great interest to study the mechanisms of NO reduction by nitrogenous species in pyrolysis gas, as this may help optimize the operating conditions that would decrease NO_x emissions during coal combustion.

Based on previous works, there are two types of nitrogenous species in coal pyrolysis gas, which are hydrogen cyanide (HCN) and ammonia (NH₃) [8,9]. NO is chosen as the target molecule in this study, as it accounts for about 95% of NO_x emissions [10,11]. Regarding NO removal by NH₃, its mechanisms have been studied for a long time in the selective non-catalytic reduction (SNCR), where NH₃ is used to decrease NO_x emissions in flue gas under fuel lean conditions [12,13]. Results indicated that reactions of NO and NH₂ radicals arising from NH₃ are the principal pathway for NO abatement. However, as temperature increases, the active OH, O and H radicals rise, leading to the oxidation of NH₃ molecules, and producing NO eventually. Consequently, there is an optimal temperature where the amount of NO reaches the lowest point. However, the NO reduction process in the reburning zone is under fuel rich conditions, which may affect the performance of NH₃ in the process of reducing NO. Moreover, there is a lack of understanding of the underlying mechanisms of NO reduction with HCN till now. Accordingly, it is of necessity and importance to explore the fundamental mechanisms of NO reduction by HCN and NH₃, respectively.

To obtain a deeper understanding of how NO molecules are converted to N₂ by HCN and NH₃, the reaction pathways of HCN and NH₃, especially on the NO consumption and N₂ formation, during the reduction process are investigated. Nonetheless, it is costly and difficult to examine intermediates by experimental studies due to the limitations of current measurement methods. Computational approaches can be developed to overcome these problems. Quantum mechanics (QM) methods are able to study chemical reactions but the computational costs are extremely high to simulate large systems [14]. Molecular dynamics (MD) methods can simulate atomistic dynamics with reasonable computational costs, however they are conventionally formulated for the physical process rather than the chemical kinetics [15]. To resolve these issues of QM and MD methods, an attractive alternative method called the reactive force field (ReaxFF) molecular dynamics (MD) is developed combin-

ing features of QM and MD, which can simulate complex chemical reactions at affordable computational costs [16–18].

In this study, ReaxFF MD simulations are carried out to study fundamental mechanisms of NO removal by HCN and NH₃ under different temperatures. Time evolutions of main reactants (NO, HCN and NH₃) and products (N₂) are studied first. Then, the mechanisms of NO removal by HCN and NH₃ are explored at different temperatures, and the temperature influence on NO reduction performance is explained at atomic level. Finally, we compare the NO control performance between HCN and NH₃, and propose preferred operating conditions to improve NO_x reduction efficiency.

2. Methods

2.1. Reactive force field (ReaxFF) molecular dynamics (MD) simulation

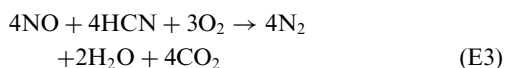
ReaxFF employs a bond-order formalism in conjunction with polarisable charge descriptions to describe both reactive and non-reactive interactions between atoms, which allows ReaxFF to accurately model both covalent and electrostatic interactions for a diverse range of materials [19]. The function of potential energy can be calculated as [20]:

$$E_{\text{system}} = E_{\text{bond}} + E_{\text{over}} + E_{\text{under}} + E_{\text{lp}} + E_{\text{val}} + E_{\text{tor}} + E_{\text{vdW}} + E_{\text{Coulomb}} \quad (\text{E1})$$

where E_{system} , E_{bond} , E_{over} , E_{under} , E_{lp} , E_{val} , E_{tor} , E_{vdW} , and E_{Coulomb} represent total energy, bond energy, overcoordination, energy penalty, undercoordination stability, lone pair energy, valence angle energy, torsion angle energy, van der Waals energy, and Coulomb energy, respectively [20].

2.2. Simulation details

All the simulations are performed with the REAXC package in LAMMPS software (Large-scale Atomic/Molecular Massively Parallel Simulator) [21,22] with C/H/O/N force field parameters [23,24]. Two three-dimensional and cubic systems with different sizes are established at the same density of 0.15 g/cm³, and the configurations are 120NO/120HCN/90O₂ and 120NO/120NH₃/30O₂ to study the reactions of NO removal by HCN and NH₃, respectively. The periodic boundary conditions are chosen in all three directions. The equivalence ratios of reactants are calculated considering the reduction equation as follows:



The canonical ensemble (NVT) [25] is selected for ReaxFF MD simulations with the Nosé-Hoover thermostat employing a damping constant of 100fs. The time step employed in this study is 0.1fs, which has been proven to be sufficiently small. At the beginning, every system undergoes energy minimization and equilibration for 20 ps at 40 K to optimize the initial geometric configuration that would otherwise cause simulation collapses. Then, the systems are heated to final temperatures ranging from 2400 to 3400 K with an increment of 200 K and then kept constant at final temperatures. The total simulation time is 1000 ps for all the simulations. The temperature employed in this study is higher than those in experiments. The adoption of a higher temperature is a common practice in MD to ensure manageable computation costs, as mentioned in [23,24].

Three replica simulations are conducted for every case with a unique starting configuration, and thus 36 simulations have been carried out and analysed in the current study. The bond order cutoff is 0.3 to recognize intermediates formed during ReaxFF MD simulations. The reactions are analysed using Chemical Trajectory Analyzer (ChemTrayzer) scripts [26]. The net flux (NF) indicates how often the reaction was observed during the simulation time, which is calculated by the number of times the direct reaction occurred minus the number of times the reverse reaction happened [27].

3. Results

3.1. Comparison of NO reduction by HCN and NH₃

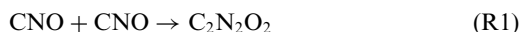
As shown in Fig. 1a and b, the consumption rates of HCN and NH₃ increase remarkably with temperature rising and NH₃ molecules are consumed faster than HCN at all temperatures. As to NO molecules, higher temperature shows better NO reduction performance by NH₃. However, the final values of NO almost remain the same in HCN environment at 2400K-3000 K, and the final amount of NO removal by HCN decreases as temperature increases when temperature is higher than 3000 K. Besides, according to Fig. 1e and f, the production of N₂ increases as temperature rises in both cases and the production of N₂ is more by NH₃ rather than HCN. The above results indicate NH₃ presents better NO reduction performance than HCN. To acquire a better understanding of NO removal by HCN and NH₃, reaction pathways are scrutinized in Sections 3.2 and 3.3, respectively.

3.2. Mechanisms of NO removal by HCN

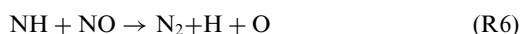
Fig. 2 reveals the mechanisms of NO reduction by HCN at 2400K-3400 K. Overall, high tempera-

tures promote new pathways of N₂ formation such as the conversion from N, HN₂ and CN₂O₂ to N₂ at 2600K-3400 K and NH to N₂ at 3400 K. During the process of NO reduction with HCN, there are three different contributions of HCN to NO removal.

The first pathway is that HCN molecules are oxidized to NO through the channel HCN → CN → CNO₂ → NO, causing negative influence on NO reduction. The second way is N₂ formation by pathways HCN → CHNO → CNO → C₂N₂O₂ → N₂ and HCN → CHNO → CNO → C₂N₂O₂ → CN₂O → N₂. Among them, the important intermediate C₂N₂O₂ is generated by the reaction:



The CNO intermediates are from the oxidation of HCN. Therefore, though N₂ is formed in this process, there is no contribution to NO removal. In the third pathway, HCN molecules undergo oxidation and decomposition forming radicals N, NH and CNO, which will further react with NO via R2 to R7 generating N₂ finally.



In addition to R6 and R7, the main reactions of N₂ formation from N₂O, HN₂O, CN₂O, C₂N₂O₂, CN₂O₂ and HN₂ during NO removal with HCN are as follows:



To further identify how temperature affects the amount of NO consumption and N₂ formation, the NFs of main elementary reactions linked with N₂ and NO are investigated in Tables 1 and 2.

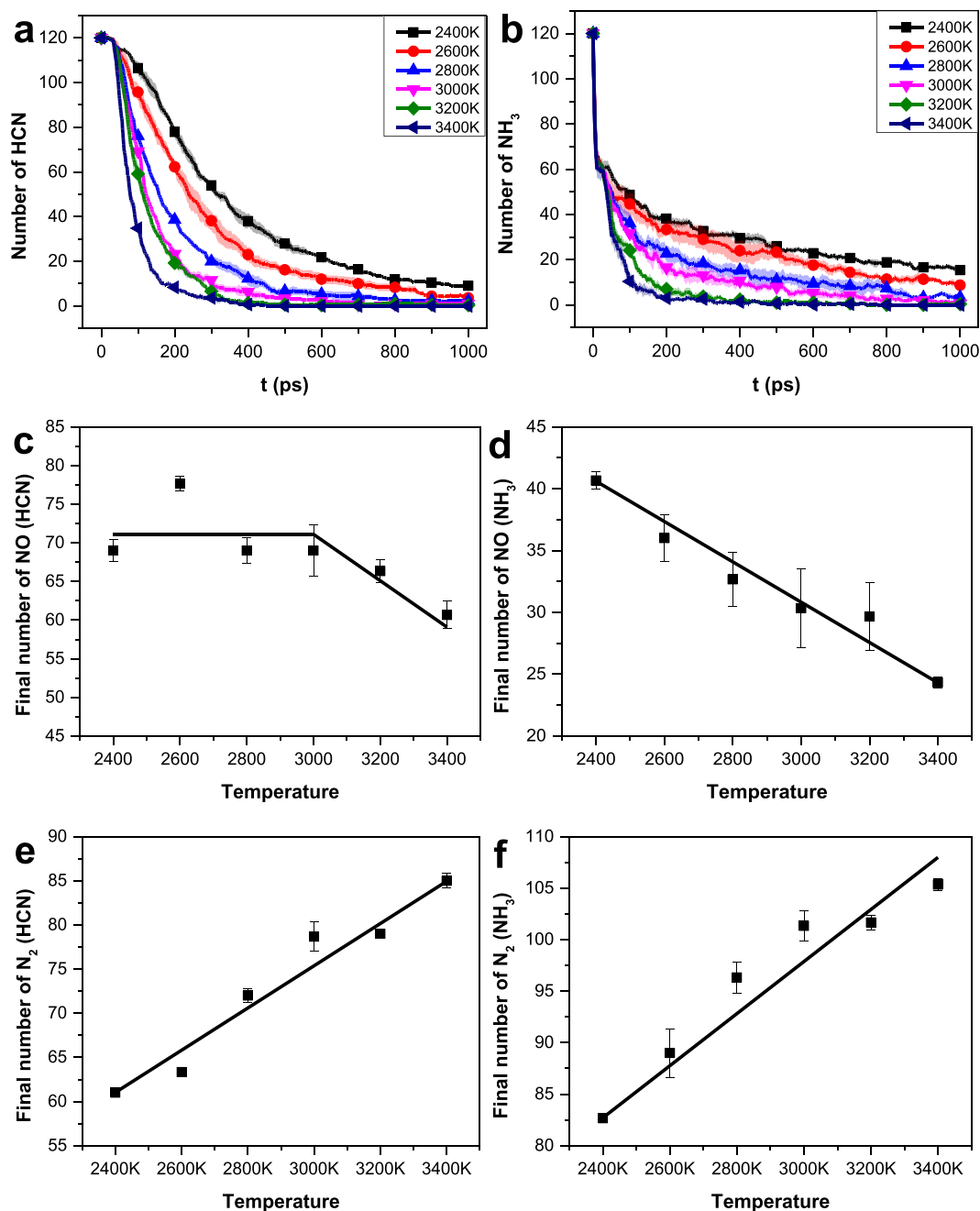


Fig. 1. Time evolution of reducing agents and final number of main products ($t = 1000$ ps) during NO removal process. (a) HCN; (b) NH_3 ; (c) NO in HCN environment; (d) NO in NH_3 environment; (e) N_2 in HCN environment; (f) N_2 in NH_3 environment.

According to Table 1, it can be noticed that the total NF of NO reduction almost remains the same at 2400K-3000 K, and increases when the temperature is higher than 3000 K. That agrees with the changes of NO numbers at different temperatures as shown in Fig. 1c. Besides, the formation and re-

duction of NO take place simultaneously during NO removal with HCN. On the whole, the NF of NO reduction presents an upward trend with increasing temperature through the promotion of reactions between NO and NH_3 as well as N (R4-R7). There is no significant enhancement of the

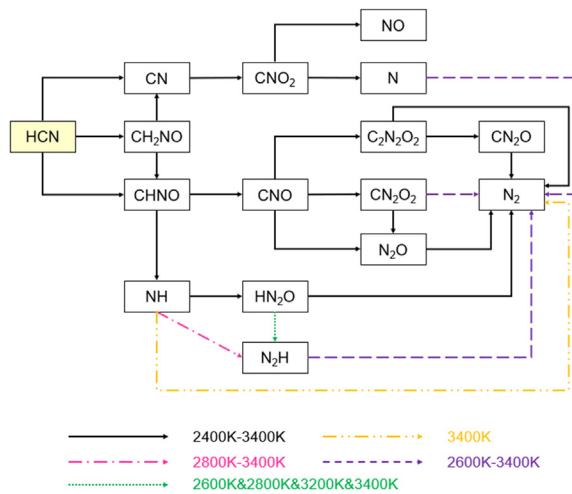


Fig. 2. Transfer pathways of NO reduction with HCN. HCN in the yellow box is the starting species.

Table 1

Net flux (NF) of main elementary pathways for NO consumption and formation during NO removal with HCN at 2400 K to 3400 K.

Pathways	2400K	2600K	2800K	3000K	3200K	3400K
CNO \rightarrow CN ₂ O ₂	46	54	34	46	48	43
CNO \rightarrow N ₂ O	15	19	25	18	20	18
NH \rightarrow HN ₂ O	11	13	15	17	12	21
N \rightarrow N ₂	0	5	8	6	9	12
NH \rightarrow N ₂ H	0	0	11	11	6	7
NH \rightarrow N ₂	0	0	0	0	0	12
NO consumption	72	91	93	98	95	113
CNO ₂ \rightarrow NO	37	51	57	60	43	55
Total consumption	35	40	36	38	52	58

Table 2

Net flux (NF) of main elementary pathways for N₂ formation during NO removal with HCN at 2400 K to 3400 K.

Pathways	2400K	2600K	2800K	3000K	3200K	3400K
N ₂ O \rightarrow N ₂	39	40	36	54	50	44
HN ₂ O \rightarrow N ₂	13	15	14	19	9	6
CN ₂ O \rightarrow N ₂	17	14	19	19	21	15
C ₂ N ₂ O ₂ \rightarrow N ₂	11	12	10	19	11	14
CN ₂ O ₂ \rightarrow N ₂	0	11	13	17	30	30
N \rightarrow N ₂	0	5	8	6	9	12
N ₂ H \rightarrow N ₂	0	6	15	8	11	13
NH \rightarrow N ₂	0	0	0	0	0	12
Total	80	103	115	142	141	146

reactions of NO and CNO. Regarding the NO generation, it is from the decomposition of CNO₂ via R16.



The NF of R16 shows the parabolic trend and peaks at 3000 K, which is the main reason why the number of NO almost remains the same at 2400K-3000 K.

Table 2 displays the NF of main elementary pathways for N₂ formation under NO reduction

with HCN conditions. The total NF of N₂ formation increases remarkably with temperature rising, accounting well for the upward trend of N₂ amount at 2400–3400 K. Specifically, the increase of N₂ production is mainly owing to the strengthening of pathways CN₂O₂ \rightarrow N₂ (R13), N \rightarrow N₂ (R7), N₂H \rightarrow N₂ (R14&R15) and NH \rightarrow N₂ (R6).

To sum up, when the temperature increases, the NO consumption and N₂ generation rise through the enhancement of the following reaction pathways: a. HCN \rightarrow CN \rightarrow CNO₂ \rightarrow N \rightarrow N₂

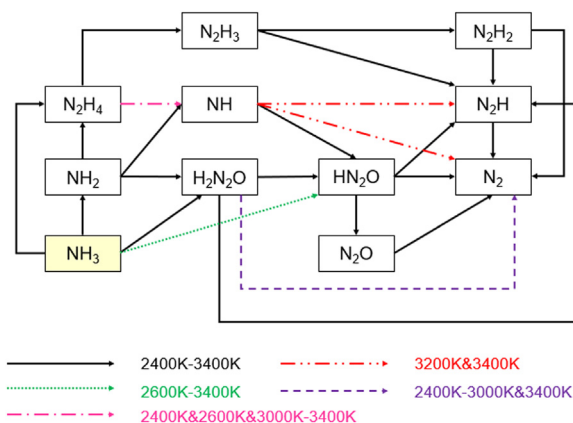
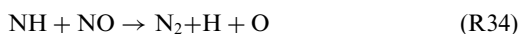
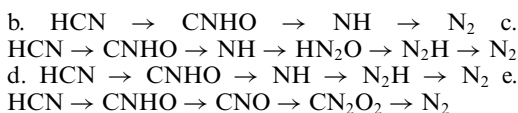
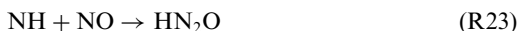
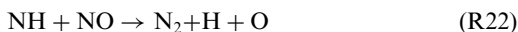
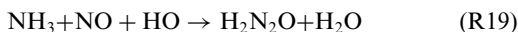
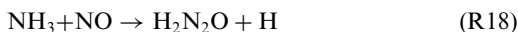
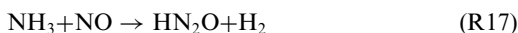


Fig. 3. Transfer pathways of NO reduction with NH_3 . NH_3 in the yellow box is the starting species.

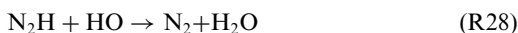


3.3. Mechanisms of NO removal by NH_3

As observed in Fig. 3, the main intermediates for NO abatement are NH_3 , NH_2 and NH by reactions R17-R34. And R17 only occurs at 2600K-3400 K.

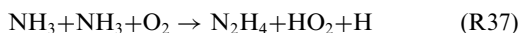


The N_2 molecules are generated by reactions as follows:



Among them, the channel $\text{NH} \rightarrow \text{N}_2$ occurs at 3200K-3400 K and $\text{H}_2\text{N}_2\text{O} \rightarrow \text{N}_2$ happens when temperatures are 2400K-3000 K and 3400 K. Besides, the pathways of N_2 formation via $\text{NH}_3 \rightarrow \text{NH}_2 \rightarrow \text{H}_2\text{N}_2\text{O} \rightarrow \text{N}_2$ and $\text{NH}_3 \rightarrow \text{NH}_2 \rightarrow \text{H}_2\text{N}_2\text{O} \rightarrow \text{N}_2\text{H} \rightarrow \text{N}_2$ are also confirmed by previous studies [12,13].

Moreover, there are also channels of N_2 generation from ammonia molecules without NO reduction. Firstly, intermediate N_2H_4 is formed by R35-R36, which will be converted to N_2 through channels $\text{N}_2\text{H}_4 \rightarrow \text{N}_2\text{H}_3 \rightarrow \text{N}_2\text{H} \rightarrow \text{N}_2$ and $\text{N}_2\text{H}_4 \rightarrow \text{N}_2\text{H}_3 \rightarrow \text{N}_2\text{H}_2 \rightarrow \text{N}_2$.



To further clarify the temperature influence on the final amount of NO and N_2 , we explore the contributions of pathways linked with NO abatement and N_2 formation under various temperatures as shown in Tables 3 and 4. The total NF of N_2 formation and NO consumption increases with temperature rising, which is in consistency with the yields of NO and N_2 at 2400K-3400 K.

As indicated in Table 3, the conversion from $\text{NH} \rightarrow \text{HN}_2\text{O}$ via R23 has an overwhelmingly dominant contribution to the increase of NO consumption with rising temperature. And the channel $\text{NH}_2 \rightarrow \text{H}_2\text{N}_2\text{O}$ via R20 plays a vital role in NO reduction especially when the temperature is in the range of 2400K-3000 K. In addition, high temperatures have a negative impact on the reaction between NH_2 and NO. The pathways $\text{NH} \rightarrow \text{N}_2\text{H}$

Table 3

Net flux (NF) of main elementary pathways for NO consumption during NO removal with NH₃ at 2400 K to 3400 K.

Pathways	2400K	2600K	2800K	3000K	3200K	3400K
NH → HN ₂ O	12	16	31	34	35	47
NH ₃ → H ₂ N ₂ O	18	16	16	18	26	21
NH ₂ → H ₂ N ₂ O	71	69	65	60	27	34
NH ₃ → HN ₂ O	0	4	5	7	3	7
NH → HN ₂	0	0	0	0	16	15
NH → N ₂	0	0	0	0	7	13
Total	101	105	117	119	114	137

Table 4

Net flux (NF) of main elementary pathways for N₂ formation during NO removal with NH₃ at 2400 K to 3400 K.

Pathways	2400K	2600K	2800K	3000K	3200K	3400K
HN ₂ O → N ₂	41	46	53	53	57	49
N ₂ H → N ₂	50	60	58	58	72	78
N ₂ H ₂ → N ₂	13	11	20	18	24	17
N ₂ O → N ₂	11	15	9	15	13	20
H ₂ N ₂ O → N ₂	13	3	8	18	0	7
NH → N ₂	0	0	0	0	7	13
Total	128	135	148	162	173	184

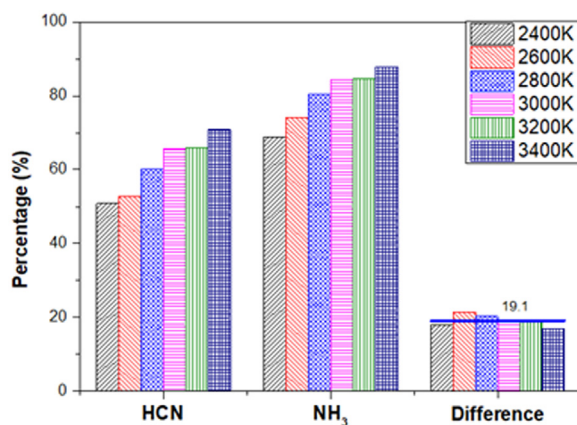


Fig. 4. Reduction efficiency of nitrogen-containing reactants.

through R21 and $\text{HN} \rightarrow \text{N}_2$ through R22 are enhanced at 3200K-3400 K.

As to N₂ formation, the pathways $\text{HN}_2\text{O} \rightarrow \text{N}_2$ via R25-R26 and $\text{N}_2\text{H} \rightarrow \text{N}_2$ via R27-R29 are promoted when the temperature ranges from 2400 K to 3400 K. There is a slight increase for channel $\text{N}_2\text{H}_2 \rightarrow \text{N}_2$ through R30 at 2400K-3400 K. As to the channel $\text{N}_2\text{O} \rightarrow \text{N}_2$ by R31, its contribution of N₂ formation almost remains the same from 2400 K to 3200 K, and increases when the temperature is 3400 K. The channel $\text{NH} \rightarrow \text{N}_2$ via R34 is strengthened at 3200K-3400 K.

Based on the above analysis, it can be concluded that high temperature promotes N₂ formation and NO consumption and NO reduction with NH₃ by pathways: f. $\text{NH}_3 \rightarrow \text{NH} \rightarrow \text{HN}_2\text{O} \rightarrow \text{N}_2$ g. $\text{NH}_3 \rightarrow \text{NH} \rightarrow \text{N}_2\text{H} \rightarrow \text{N}_2$ h. $\text{NH}_3 \rightarrow \text{NH} \rightarrow \text{N}_2$

4. Discussion

In this research, we use ReaxFF MD simulations to investigate fundamental reaction mechanisms of NO removal with HCN and NH₃ under different temperatures, which play a dominant role in NOx reduction during fuel staging with coal pyrolysis gas. To provide guidance on the reduction of NOx emissions, it is important to compare performance of NO reduction by HCN and NH₃ in the context of the existing literature.

Regarding the NOx control performance, the number of NO molecules is adopted to indicate the removal efficiency in previous studies [12,13,28,29]. On the other hand, in addition to NO, the remaining nitrogen-containing species in the system will be oxidized to NOx in the subsequent burnout

zone, causing pollution to the environment. Therefore, in this study, the number of N_2 produced is used as an indicator to reflect the reduction efficiency of nitrogen-containing reactants as shown in Fig. 4. It is clear that the NOx control performance is promoted by rising temperature in both cases, and NH_3 shows about 19.1% higher capability than HCN for the NO reduction from 2400 K to 3400 K. Moreover, the optimal temperature is not observed in our simulations during NO removal by NH_3 , which is inconsistent with the phenomena in SNCR process using ammonia [12,13,28,29]. That is because the SNCR process is operated under excess oxygen conditions, and high temperature promotes the oxidation of NH_3 forming NO, resulting in the lowered performance of NO reduction. However, NO molecules are consumed under fuel rich conditions in the reburning zone, and the oxidation of nitrogenous intermediates is suppressed at high temperatures. Thus, the behaviours of NO reduction with NH_3 are not inhibited with temperatures rising.

Base on the above analysis, the increase of the reaction temperature is an effective method to improve the NOx reduction performance of coal pyrolysis gas. In addition, promotion of the conversion from HCN to NH_3 during reduction process also benefits the decrease of NOx pollutants, which can be achieved by increasing temperature, pressure and moisture during coal pyrolysis [8,9]. To obtain better control strategies for staging combustion with pyrolysis gas, extended simulations with different reducing agents and oxygen contents are required.

5. Conclusions

ReaxFF simulations are performed to explore the mechanisms of NO removal by HCN and NH_3 with temperature ranging from 2400 K to 3400 K, respectively. Based on the analysis of simulation results, the following conclusions can be drawn:

- (1) There are three different contributions of HCN during NO removal. The first pathway is that HCN molecules are oxidized to NO through $HCN \rightarrow CN \rightarrow CNO_2 \rightarrow NO$. The second way is N_2 formation by pathways $HCN \rightarrow CHNO \rightarrow CNO \rightarrow C_2N_2O_2 \rightarrow N_2$ and $HCN \rightarrow CHNO \rightarrow CNO \rightarrow C_2N_2O_2 \rightarrow CN_2O \rightarrow N_2$, where there is no contribution to NO consumption and production. In the final way, the NO molecules react with intermediates (CNO, N and NH) from HCN generating N_2 eventually.
- (2) As to NH_3 molecules, part of them directly generates N_2 without coupling with NO via $NH_3/NH_2 \rightarrow N_2H_4 \rightarrow N_2H_3 \rightarrow N_2H \rightarrow N_2$ and $NH_3/NH_2 \rightarrow N_2H_4 \rightarrow N_2H_3 \rightarrow N_2H_2 \rightarrow N_2$. In addition, N_2 formation can also come

from the reactions between NO and nitrogen-containing particles (like NH_3 , NH_2 and NH).

- (3) NH_3 is about 19.1% more capable of NO reduction than HCN at 2400K-3400 K. The NO reduction performance is promoted by rising temperature under both HCN and NH_3 conditions via pathways:
 - a $HCN \rightarrow CN \rightarrow CNO_2 \rightarrow N \rightarrow N_2$
 - b $HCN \rightarrow CNHO \rightarrow NH \rightarrow N_2$
 - c $HCN \rightarrow CNHO \rightarrow NH \rightarrow HN_2O \rightarrow N_2H \rightarrow N_2$
 - d $HCN \rightarrow CNHO \rightarrow NH \rightarrow N_2H \rightarrow N_2$
 - e $HCN \rightarrow CNHO \rightarrow CNO \rightarrow CN_2O_2 \rightarrow N_2$
 - f $NH_3 \rightarrow NH \rightarrow HN_2O \rightarrow N_2$
 - g $NH_3 \rightarrow NH \rightarrow N_2H \rightarrow N_2$
 - h $NH_3 \rightarrow NH \rightarrow N_2$

This research provides new insight into the mechanisms of NO reduction with nitrogen-containing species (HCN and NH_3) in coal pyrolysis gas, which may lead to guidance on the optimization of run conditions that would increase the NOx control performance.

Declaration of Competing Interest

The authors declare that they have no known competing financial interests or personal relationships that could have appeared to influence the work reported in this paper.

Acknowledgements

Support from the UK Engineering and Physical Sciences Research Council under the project "UK Consortium on Mesoscale Engineering Sciences (UKCOMES)" (Grant No. EP/R029598/1) is gratefully acknowledged. This work made use of computational support by CoSeC, the Computational Science centre for Research Communities, through UKCOMES.

References

- [1] C.T. Bowman, *Symp. (Int.) Combust.* 24 (1992) 859–878.
- [2] T. Luan, X. Wang, Y. Hao, L. Cheng, *Appl. Energ* 86 (2009) 1783–1787.
- [3] R. Bilbao, A. Millera, M.U. Alzueta, L. Prada, *Fuel* 76 (1997) 1401–1407.
- [4] J. Smart, D. Morgan, *Fuel* 73 (1994) 1437–1442.
- [5] H. Liu, E. Hampartsoumian, B.M. Gibbs, *Fuel* 76 (1997) 985–993.
- [6] U. Greul, H. Spliethoff, H.-C. Magel, et al., *Symp. (Int.) Combust.* 26 (1996) 2231–2239.
- [7] H. Rüdiger, U. Greul, H. Spliethoff, K.R. Hein, *Fuel* 76 (1997) 201–205.
- [8] J. Liu, X. Guo, *Fuel. Process. Technol* 161 (2017) 107–115.

- [9] Z. Bai, X.Z. Jiang, K.H. Luo, *Energy* 238 (2022) 121798.
- [10] P. Glarborg, A. Jensen, J.E. Johnsson, *Prog. Energ. Combust* 29 (2003) 89–113.
- [11] Z. Wang, J. Zhou, Y. Zhu, Z. Wen, J. Liu, K. Cen, *Fuel. Process. Technol* 88 (2007) 817–823.
- [12] S.J. Klippenstein, L.B. Harding, P. Glarborg, J.A. Miller, *Combust. Flame* 158 (2011) 774–789.
- [13] Q. Cao, H. Liu, S.-H. Wu, L.-P. Zhao, X. Huang, *2008 2nd International Conference on Bioinformatics and Biomedical Engineering* (2008) 4034–4038.
- [14] M. Feng, X.Z. Jiang, K.H. Luo, *P. Combust. Inst* 37 (2019) 5473–5480.
- [15] X.Z. Jiang, K.H. Luo, Y. Ventikos, *Acta. Physiol.* 228 (2020) e13376.
- [16] X.Z. Jiang, M. Feng, W. Zeng, K.H. Luo, *P. Combust. Inst.* 37 (2019) 5525–5535.
- [17] M. Feng, X.Z. Jiang, W. Zeng, K.H. Luo, *P. Hellier, Fuel* 235 (2019) 515–521.
- [18] X.Z. Jiang, K.H. Luo, *P. Combust. Inst.* 38 (2021) 6605–6613.
- [19] T.P. Senftle, S. Hong, M.M. Islam, et al., *npj. Comput. Mater.* 2 (2016) 1–14.
- [20] C. Ashraf, A.C. Van Duin, *J. Phys. Chem. A* 121 (2017) 1051–1068.
- [21] H.M. Aktulga, J.C. Fogarty, S.A. Pandit, A.Y. Grama, *Parallel. Comput.* 38 (2012) 245–259.
- [22] S. Plimpton, *J. Comput. Phys.* 117 (1995) 1–19.
- [23] L. Zhang, A.C.V. Duin, S.V. Zybin, W.A. Goddard III, *J. Phys. Chem. B* 113 (2009) 10770–10778.
- [24] L. Zhang, S.V. Zybin, A.C. Van Duin, S. Dasgupta, W.A. Goddard III, E.M. Kober, *J. Phys. Chem. A* 113 (2009) 10619–10640.
- [25] H.C. Andersen, *J. Chem. Phys.* 72 (1980) 2384–2393.
- [26] M. Döntgen, M.-D. Przybylski-Freund, L.C. Kröger, W.A. Kopp, A.E. Ismail, K. Leonhard, *J. Chem. Theory. Comput.* 11 (2015) 2517–2524.
- [27] S. Arvelos, C.E. Hori, *J. Chem. Inf. Model* 60 (2020) 700–713.
- [28] S.W. Bae, S.A. Roh, S.D. Kim, *Chemosphere* 65 (2006) 170–175.
- [29] C. Locci, L. Vervisch, B. Farcy, P. Domingo, N. Perret, *Flow. Turbul. Combust.* 100 (2018) 301–340.